Article

Variable Density Effect of Self-Assembled Polarizable Monolayers on the Electronic Properties of Silicon

Naama Peor, Ruthy Sfez, and Shlomo Yitzchaik

J. Am. Chem. Soc., **2008**, 130 (12), 4158-4165 • DOI: 10.1021/ja077933g

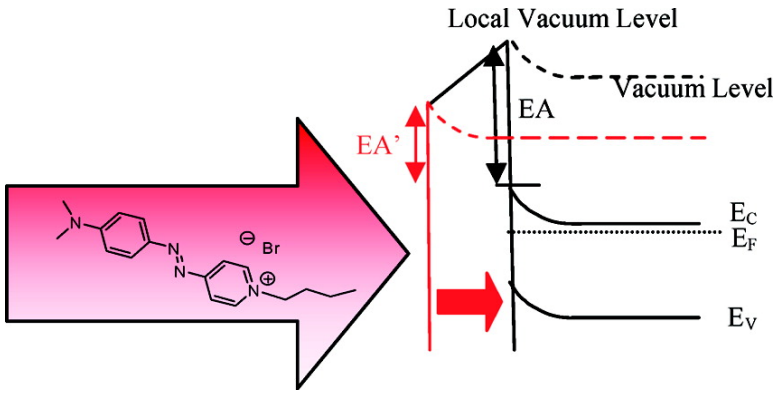

More About This Article

Additional resources and features associated with this article are available within the HTML version:

- Supporting Information
- Access to high resolution figures
- Links to articles and content related to this article
- Copyright permission to reproduce figures and/or text from this article

View the Full Text HTML

J|A|C|S
ARTICLES
Published on Web 03/04/2008

Variable Density Effect of Self-Assembled Polarizable Monolayers on the Electronic Properties of Silicon

Naama Peor, Ruthy Sfez, and Shlomo Yitzchaik*

The Institute of Chemistry and the Hebrew University Center for Nanoscience and Nanotechnology, The Hebrew University of Jerusalem, Jerusalem 91904, Israel

Received October 16, 2007; E-mail: sy@cc.huji.ac.il

Abstract: Electronic structures at the Si/SiO_2/molecule interfaces were studied by Kelvin probe techniques (contact potential difference) and compared to theoretical values derived by the Helmholtz equation. Two parameters influencing the electronic properties of n-type <100> Si/SiO_2 substrates were systematically tuned: the molecular dipole of coupling agent molecules comprising the layer and the surface coverage of the chromophoric layer. The first parameter was checked using direct covalent grafting of a series of trichlorosilane-containing coupling agent molecules with various end groups causing a different dipole with the same surface number density. It was found that the change in band bending (ΔBB) clearly indicated a major effect of passivation due to two-dimensional polysiloxane network formation, with minor differences resulting from the differences in the end groups' capacity to act as "electron traps". The change in electron affinity (ΔEA) parameter increased upon increasing the dipole of the end group comprising the monolayer, resulting in a range of 600 mV. Moreover, a shielding effect of the aromatic spacer compared with the aliphatic spacer was found and estimated to be about 200 mV. The density effect was examined using the 4-[4-(*N*,*N*-dimethylamino phenyl)azo]pyridinium halide chromophore which has a calculated dipole of more than 10 D. It was clearly shown that upon increasing surface chromophoric coverage an increase in the electronic effects on the Si substrate was observed. However, a major consequence of depolarization was also detected while comparing the experimental and calculated values.

Introduction

The adsorption of organic molecules on inorganic semiconductors substrates has attracted increasing interest in past decades due to their ability to control and tune the electronic properties of semiconductors and metal surfaces;[1−23] ergo, device performances can be tuned.[24−32] Polar molecules are often used to modify electronic properties such as barrier height values[1−6] and work functions (WF).[7−10] The chemical functionality directed from the surface up has a crucial influence on the resulting surface properties, both structurally and electronically.[11] Indeed, it was already shown that organic self-

(1) Vilan, A.; Cahen, D. *Trends Biotechnol.* **2002**, *20*, 22−29.
(2) Haick, H.; Ambrico, M.; Ligonzo, T.; Tung, R. T.; Cahen, D. *J. Am. Chem. Soc.* **2006**, *128*, 6854−6869.
(3) Vilan, A.; Shanzer, A.; Cahen, D. *Nature* (*London*) **2000**, *404*, 166−168.
(4) Ashkenasy, G.; Cahen, D.; Cohen, R.; Shanzer, A.; Vilan, A. *Acc. Chem. Res.* **2002**, *35*, 121−128.
(5) Zuppiroli, L.; Si-Ahmed, L.; Kamaras, K.; Nüsch, F.; Bussac, M. N.; Ades, D.; Siove, A.; Moons, E.; Grätzel, M. *Eur. Phys. J. B* **1999**, *11*, 505.
(6) Crispin, X.; Geskin, V.; Crispin, A.; Cornil, J.; Lazzaroni, R.; Salaneck, W. R.; Bredas, J. L. *J. Am. Chem. Soc.* **2002**, *124*, 8131−8141.
(7) Krüger, J.; Bach, U.; Grätzel, M. *Adv. Mater.* **2000**, *12*, 447−451.
(8) Ofir, Y.; Zenou, N.; Goykhman, I.; Yitzchaik, S. *J. Phys. Chem. B* **2006**, *101*, 8002−8009.
(9) Nuesch, F.; Rotzinger, F.; Si-Ahmed, L.; Zuppiroli, L. *Chem. Phys. Lett.* **1998**, *288*, 861−867. Ganzorig, C.; Kwak, K.-J.; Yagi, K.; Fujihira, M. *Appl. Phys. Lett.* **2001**, *79*, 272−274. Rudich, Y.; Benjamin, I.; Naaman, R.; Thomas, E.; Trakhtenberg, S.; Ussyshkin, R. *J. Phys. Chem. A* **2000**, *104*, 5238−5245. Linford, M. R.; Fenter, P.; Eisenberger, P. M.; Chidsey, C. E. D. *J. Am. Chem. Soc.* **1995**, *117*, 3145−3155.
(10) Si-Ahmed, L.; Nüesch, F.; Zuppiroli, L.; François, B. *Macromol. Chem. Phys.* **1998**, *199*, 625−632.
(11) Ulman, A. *Chem. Rev.* **1996**, *96*, 1533−1554. Ulman, A. *An Introduction to Ultrathin Organic Films*; Academic Press: Boston, 1991. Kronik, L.; Shapira, Y. *Surf. Sci. Rep.* **1999**, *37*, 1−299.
(12) Cohen, R.; Zenou, N.; Cahen, D.; Yitzchaik, S. *Chem. Phys. Lett.* **1997**, *279*, 270−274. Zenou, N.; Zelichenok, A.; Yitzchaik, S.; Cohen, R.; Cahen, D. *ACS Symp. Ser.* **1997**, *695*, 57−66.
(13) Sfez, R.; Peor, N.; Cohen, S. R.; Cohen, H.; Yitzchaik, S. *J. Mater. Chem.* **2006**, *16*, 4044−4050.
(14) Ray, S. G.; Cohen, H.; Naaman, R.; Liu, H.; Waldeck, D. H. *J. Phys. Chem. B* **2005**, *109*, 14064−14073.
(15) Cohen, R.; Kronik, L.; Shanzer, A.; Cahen, D.; Liu, A.; Rosenwaks, Y.; Lorenz, J. K.; Ellis, A. B. *J. Am. Chem. Soc.* **1999**, *121*, 10545−10553.
(16) Cohen, R.; Kronik, L.; Vilan, A.; Shanzer, A.; Rosenwaks, Y.; Cahen, D. *Adv. Mater.* **2000**, *12*, 33−37.
(17) Cahen, D.; Kahn, A.; Umbach, E. *Mater. Today* **2005**, *8*, 32−41.
(18) Cui, Y.; Lieber, C. M. *Science* **2001**, *291*, 851−853.
(19) Ishii, H.; Sugiyama, K.; Ito, E.; Seki, K. *Adv. Mater.* **1999**, *11*, 605−625.
(20) Saito, N.; Hayashi, K.; Sugimura, H.; Takai, O. *Langmuir* **2003**, *19*, 10632−10634.
(21) Reed, M. A.; Tour, J. M. *Appl. Phys. Lett.* **2000**, *77*, 1224.
(22) Iozzi, M. F.; Cossi, M. *J. Phys. Chem. B* **2005**, *109*, 15383−15390.
(23) Seker, F.; Meeker, K.; Kuech, T. F.; Ellis, A. B. *Chem. Rev.* **2000**, *100*, 2505−2536.
(24) Wu, D. G.; Ashkenasy, G.; Shvarts, D.; Ussyshkin, R. V.; Naaman, R.; Shanzer, A.; Cahen, D. *Angew. Chem., Int. Ed.* **2000**, *39*, 4496−4500.
(25) Wu, D. G.; Cahen, D.; Graf, P.; Naaman, R.; Nitzan, A.; Shvarts, D. *Chem.—Eur. J.* **2001**, *7*, 1743−1749.
(26) Cahen, D.; Naaman, R.; Vager, Z. *Adv. Funct. Mater.* **2005**, *15*, 1571−1578.
(27) Patolsky F.; Zheng, G. F.; Lieber, C. M. *Anal. Chem.* **2006**, *78*, 4260−4269 and references therein.
(28) Niwa, D.; Yamada, Y.; Homma, T.; Osaka, T. *J. Phys. Chem. B* **2004**, *108*, 3240−3245.
(29) Rampi, M. A.; Whitesides, G. M. *Chem. Phys.* **2002**, *281*, 373−391.
(30) Salomon, A.; Cahen, D.; Lindsay, S.; Tomfohr, J.; Engelkes, V. B.; Frisbie, C. D. *Adv. Mater.* **2004**, *16*, 477.
(31) Shen, Y.; Hosseini, A. R.; Wong, M. H.; Malliaras, G. G. *Chem. Phys. Chem.* **2004**, *5*, 16−25.
(32) Chabinyc, M. L.; Chen, X.; Holmlin, R. E.; Jacobs, H.; Skulason, H.; Frisbie, C. D.; Mujica, V.; Ratner, M. A.; Rampi, M. A.; Whitesides, G. M. *J. Am. Chem. Soc.* **2002**, *124*, 11730−11736.

10.1021/ja077933g CCC: $40.75

assembled monolayers (SAM) can tune the electronic properties of interfaces by modifying the existing surface dipole and adding an external dipole layer.[12−14] Moreover, the changes in the dipole of the adsorbed molecules are considered to be a major controlling factor in novel chemical and biological molecule-based sensing electronic and opto-electronic devices.[24,31] The change in the surface dipole can be derived experimentally by Kelvin probe analysis or theoretically by the Helmholtz equation. The Kelvin probe method is widely used to determine the relative WF of semiconductors by measuring the contact potential difference (CPD) between a reference surface and the sample. The unknown difference between the conductive/valence band and the Fermi level is eliminated by subtracting the absolute values of the sample and the reference substrate. Since the WF of a semiconductor is composed from band bending (BB) and electron affinity (EA) parameters, it is possible to determine both of them experimentally by finding the CPD.[12,13] On the other hand, the surface dipole can also be derived theoretically from the Helmholtz equation (eq 1). From eq 1 it can be seen that two parameters are of extreme importance when choosing a specific molecule for tailoring surface electronic properties, the molecular dipole (magnitude and orientation) and the density of the adsorbed molecules on the surface. Eq 1 is

$$\Delta\Phi_s = \frac{N\mu}{\epsilon\epsilon_0}\cos\theta \qquad (1)$$

where $N\mu$ is the dipole density (in m^2/molecule), μ is the dipole moment (in debye, 1 D = 3.34×10^{-30} C·m), θ is the average tilt angle of the dipole with respect to the surface normal, ϵ is the effective dielectric constant of the molecular film, and ϵ_0 is the permittivity of vacuum; here $\Delta\Phi_s$ is expressed in units of volts.

Usually, there is a factor between the calculated and the observed values, due to local environmental effects such as hydration and depolarization.[33] The depolarization influences the obtained layer a lot and should be taken into account concerning the packaging and ordering of the molecules, when the molecular dipole is greater than about 5 D.[35−37] Although many experimental and theoretical works have dealt with the influence of the dipole on the electronic properties of the substrate, almost no experimental works have been conducted with the aim to elucidate the influence of the layer's number density on the substrate. Recently, a theoretical study was conducted regarding the depolarization effects arising from different clusters sizes, aiming to predict the density effect on modeled etched <1,1,1> Si substrates.[35] Experimental work that dealt with molecular monolayers adsorbed on periodic surfaces showed a linear correlation between the lattice constant of the semiconductor and the molecular effect obtained.[4] The higher the density of the binding sites (i.e., smaller lattice constant), the higher the molecular dipoles' density, and thus the larger

Scheme 1. Covalent Assembly of Various Trichlorosilane-Containing Coupling Agents on Hydroxyl Terminated Substrates (Step 1)[a]

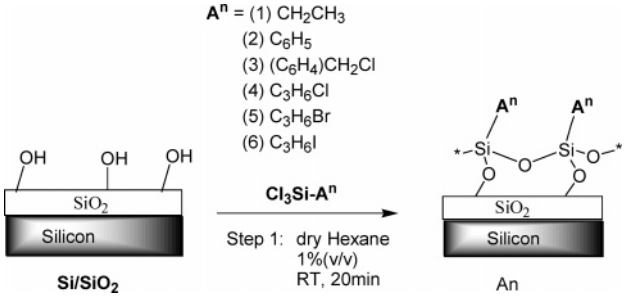

[a] A*n* stands for the free residue, while A*n* stands for the SAM.

electronic surface dipole effect obtained upon molecular assembly. Most of the literature deals with polar and dense monolayers anchored to metal and bare semiconductors surfaces without native oxides, in order to increase the influence of the layer on the electronic properties of the substrate.[38,39] Due to the fact that Si/SiO_2 is the most common interface for electronic devices, there is a great motivation to investigate the influence of organic monolayers on the electronic properties of this substrate. However, few researchers have studied oxide-bearing semiconductors as substrates[8,12,13,37,40] or as devices[41] or both,[42] indicating tuning of the electronic properties of the semiconductor even through the oxide layer. It was shown[12] that the change in the electron affinity parameter (ΔEA) in <1,0,0> Si/SiO_2 had a linear correlation with the Hammett parameter of isolated molecules in the gas phase. Moreover, it was shown that a major surface passivation occurs upon the formation of a two-dimensional (2D) polysiloxane-based monolayer on the substrate.[13] Upon application on a Si/SiO_2-based device, the ability to control the carrier density in the conduction channel of an organic field-effect transistor by the use of SAMs with a different terminal group that is characterized by a different molecular dipole was also verified.[43] It is clear that the hybrid consisting of Si substrate, native oxide, and adsorbed organic monolayer has high importance and potential in both device application and fundamental science.

In this contribution, we systematically examined the molecular variables which control the electronic properties of <1,0,0> n-type Si/SiO_2 surfaces. In order to do so, two steps of assembly were conducted on the surface. The first step involved the assembly of coupling agents baring a trichlorosilane head group with various tail groups and spacers (Scheme 1). The tail groups differ mostly by their dipole moments as was obtained from MOPAC minimization for the single molecule (Table 1). A linear fit was obtained between the changes in electronic properties of the semiconductor with what was predicted by the Helmholtz equation (Figure 3). Two spacers were examined: aliphatic vs aromatic, giving rise to an important shielding

(33) He, T.; He, J.; Lu, M.; Chen, B.; Pang, H.; Reus, W. F.; Nolte, W. M.; Nackashi, D. P.; Franzon, P. D.; Tour, J. M. *J. Am. Chem. Soc.* **2006**, *128*, 14537−14541.
(34) El-Abed, A.; Ionov, R.; Goldmann, M.; Fontaine, P.; Billard, J.; Peretti, P. *Europhys. Lett.* **2001**, *56*, 234−240.
(35) Deutsch, D.; Natan, A.; Shapira, Y.; Kronik, L. *J. Am. Chem. Soc*. **2007**, *129*, 2989−2997.
(36) Cornil, D.; Olivier, Y.; Geskin, V.; Cornil, J. *Adv. Funct. Mater*. **2007**, *17*, 1143−1148.
(37) Gershevitz, O.; Sukenik, C. N.; Ghabboun, J.; Cahen, D. *J. Am. Chem. Soc.* **2003**, *125*, 4730−4731.
(38) Hunger, R.; Jaegermann, W.; Merson, A.; Shapira, Y.; Pettenkofer, C.; Rappich, J. *J. Phys. Chem. B* **2006**, *110*, 15432−15441.
(39) Chen, J.; Reed, M. A.; Rawlett, A. M.; Tour, J. M. *Science* **1999**, *286*, 1550−1552.
(40) Gershewitz, O.; Grinstein, M.; Sukenik, C.; Regev, K.; Ghabboun, J.; Cahen, D. *J. Phys. Chem. B* **2004**, *108*, 664−672.
(41) Collier, C. P.; Wong, E. W.; Belohradsky, M.; Raymo, F. M.; Stoddart, J. F.; Kuekes, P. J.; Williams, R. S.; Heath, J. R. *Science* **1999**, *285*, 391−394.
(42) Liu, Y.; Yu, H. *Chem. Phys. Chem*. **2003**, *4*, 335−342.
(43) Kobayashi, T.; Nishikawa, T.; Takenobu, S.; Mori, T.; Shimoda, T.; Mitani, H.; Shimonati, N.; Yoshimoto, S.; Ogawa and Iwasa, Y. *Nat. Mater*. **2004**, *3*, 317−322.

Table 1. Electronic and Spectroscopic Properties of the Various Silylated Substrates

	calcd dipole [D]	contact angle [deg][a]	thickness [Å][a] calcd[a]	thickness [Å][a] ellipsometry	Δ(CPD ± 10) [mV][a] dark	Δ(CPD ± 10) [mV][a] light
SiO_2		<5		16 ± 3	0	0
A1	−0.89	82 ± 2	5.0	4.7 ± 0.3	−246	−96
A2	−0.98	74 ± 2	6.6	6.3 ± 0.4	−349	−219
A3	0.79	74 ± 2	7.9	8.1 ± 0.6	80	200
A4	1.63	75 ± 1	6.8	8.6 ± 1.4	239	379
A5	1.60	76 ± 2	7.0	6.7 ± 0.5	146	276
A6	1.47	78 ± 2	7.2	6.7 ± 0.5	142	212

[a] Statistical error statements are based on at least five different substrates.

factor in the aromatic spacer. The second step consisted of the construction of various surface coverage at the submonolayer regime, of a polarizable chromophore via an in-situ S_N2 reaction (Scheme 2). We choose 4-[4-(*N*,*N*-dimethylamino phenyl)azo]-pyridine (MAP) as the desired chromophore precursor due to the fact that upon quaternization reaction it becomes a polarizable molecule with a high calculated dipole moment (∼10 D) that can be a good candidate to induce electronic changes in the bulk Si. In the case of the dense and organized monolayer containing high molecular dipoles (>5 D), molecular layer depolarization is observed. This depolarization effect might be also expected in a less dense and organized monolayer, however, still giving rise to a notable change in the electronic properties as predicted by theory.[44] This establishes the important role played by coverage, in addition to local chemical properties, in tailoring surface chemistry via polar molecule adsorption.

The SAMs' binding onto the surface was verified by X-ray photoelectron spectroscopy (XPS), atomic force microscopy (AFM), UV−vis absorption spectra, variable-angle spectroscopic ellipsometry (VASE), and contact angle measurements. CPD equipment, using the vibrating Kelvin probe technique, was used to monitor and determine the molecular effects on the electronic properties of the silicon. The relevant properties that were evaluated are the silicon work function (WF), band-bending (BB), and electron affinity (EA). The influence of the molecular dipole and type of spacers in a SAM of coupling agent on the electronic properties of a Si/SiO_2 substrate was demonstrated. It was shown that the larger the molecular dipole, the larger the ΔEA parameter value, as was predicted by theory. Aromatic spacers induced a shielding that was estimated to be of about 200 mV in magnitude. The second layer of the MAP^+ chromophore has shown an important dependence of the surface dipole upon increase in chromophore surface number density, while preserving the shielding effect of the ring from the coupling agent layer beneath. The depolarization effect was clearly obtained for these chromophoric layers.

Experimental Section

A. General. A.1. Substrate Cleaning. Quartz (Chemglass), glass slides (Knittel Glaser), and *n*-Si <100> (Virginia Semiconductors) substrates were cleaned in aqueous detergent, rinsed copiously with triple distilled water (TDW), then dipped in hot (90 °C) piranha solution for 60 min (3:7 by volume of 30% H_2O_2 (MOS) and conc. H_2SO_4 (MOS "BAK-ANAL" REAG) (***Caution*****:** *strong oxidizing solution, handle with care*). The substrates were then rinsed with TDW and further cleaned with $H_2O/H_2O_2/NH_3$ (5:1:0.25) solution while sonicating for 15 min at 60 °C. After subsequent washing with TDW, the substrates were immersed for 5 min in pure acetone and finally dried under a stream of nitrogen.

A.2. Chemicals. A.2.a. **Coupling Agents.** Ethyltrichlorosilane, phenyltrichlorosilane, (chloromethyl)phenyltrichlorosilane, (3-chloropropyl)trichlorosilane, and (3-bromopropyl)trichlorosilane [Gelest], were vacuum distilled before use. The (3-iodopropyl)triiodosilane was synthesized immediately before use, obtained from (3-bromopropyl)-trichlorosilane.

A.2.b. Solvents. *n*-Heptane, hexanes (95% *n*-hexane ULTRA RESI analyzed) [J. T. Baker] were distilled on sodium under a nitrogen atmosphere, acetonitrile was distilled on CaH_2, *n*-propanol was used after passing alumina column. 2-Propanol, THF, dichloromethane, ethanol, acetone, chloroform, diethylether anhydrous, ethyl acetate and methanol [Aldrich] were used as received.

A.2.c. Reagents. Propyl bromide, benzyl chloride, sodium, 4-aminopyridine, *N*,*N*-dimethylaniline, tetrafloroburate acid (HBF_4 48% in water), (4-dimethylamino)pyridine, sodium iodide anhydrous, sodium nitrite, and sodium hydroxide [Aldrich] were used without further purification.

B. Synthesis of Starting Materials. B.1. Synthesis of 3-Iodopropyl Triiodosilane. An excess of sodium bromide (50 gr of NaBr) in a three-neck flask with a mechanical stirrer was left under vacuum at 60 °C overnight. Portions of 50 mL of dry CH_3CN and 3-bromopropyl triclorosilane (8.8 mmol) were added at room temperature. The mixture was stirred for 8 h. Then 100 mL of dry heptane was added, and the mixture was stirred vigorously for 5 min to extract the product. The product was transferred under ambient conditions for further surface-anchoring reaction. XPS analysis following surface adsorption showed the disappearance of the characteristic peak of bromine (binding energy 69.1 eV) and the appearance of the iodide characteristic peak (binding energy 630 and 617 eV).

B.2. Synthesis of 4-[4-(*N*,*N*-Dimethylamino Phenyl)azo]pyridine (MAP). 4-Aminopyridine (0.021 mol) was dissolved in tetrafluoroborate acid (48% water) at 0 °C, and a milky solution was then obtained. Sodium nitrite (0.021mol) was carefully added, keeping the mixture temperature at 0 °C. Dimethylaniline (0.043 mol) was added, and the mixture was stirred at room temperature. The adition of a concentrated solution of NaOH until the neutralization of the solution led to product precipitation. The residue was filtered, dissolved in minimum DCM, and then purified by column chromatography (silica gel 60, 0.2 mesh) using hexane/EtOAc (1:2, respectively) as an eluent to afford the product in 85−90% yield.

The product MAP precursor was obtained as an orange solid. ^{1}H NMR: δ 3.13(s, N(CH3)2, 6H), 6.75−6.78(dd, HAr, 2H), 7.63−7.65-(d, HAr, 2H), 7.89−7.92(d, HAr, 2H), 8.71−8.73(d, HAr, 2H). FTIR (KBr pellet): 1445, 1519, 1552, 1563, 1581, and 1603 cm^{-1}. UV−vis. λ_{max}^{EtOH} = 440 nm, $\epsilon^{\lambda_{max}}$ (MeOH) = 25 973 [cm^{-1} M^{-1}]. Anal. Calcd: 69.00 C, 6.24 H, 24.76 N. Found: 68.70 C, 6.34 H, 24.47 N.

B.3. General Synthetic Procedure for Chromophores' Models. A mixture of the precursor (MAP) in an excess of propylbromide or benzylbromide was heated under reflux for 12 h. The solid was filtered and washed under cold EtOAc. Finally, the product was recrystallized from methanol.

1-Propyl[4-(4-)*N*,*N*-dimethylamino phenyl)azo)pyridinium bromide ($PrBr\text{-}MAP^+$): ^{1}H NMR: δ 1.04−1.25(t, CH3CH2, 3H), 2.08−2.16-(sec, CH_3CH_2, 2H), 3.25(s, $N(CH_3)2$, 6H), 4.86−4.91(t, N + $-CH_2$, 2H), 6.79−6.91(dd, HAr, 2H), 7.96−7.99(d, HAr, 2H), 8.09−8.12(d, HAr, 2H), 9.22−9.24(d, HAr, 2H). FTIR (KBr pellet): 1500, 1541, 1560, 1600, and 1629 cm^{-1}. UV−vis. λ_{max}^{EtOH} = 555 nm, $\epsilon^{\lambda_{max}}$ (MeOH) = 50 149 [cm^{-1} M^{-1}]. Anal. Calcd: 55.02 C, 6.06 H, 16.04 N. Found: 54.55 C, 6.04 H, 15.72 N.

1-Benzyl[4-(4-)*N*,*N*-dimethylamino phenyl)azo)pyridinium]chloride ($BzCl\text{-}MAP^+$): ^{1}H NMR: δ 3.26(s, $N(CH_3)_2$, 6H), δ 6.25(s, HAr, 1H), 6.79−6.82(dd, HAr, 2H), 7.33−7.42(m, HAr, 2H), 7.61−7.63(dd, HAr,

(44) Natan, A.; Zidon, Y.; Shapira, Y.; Kronik, L. *Phys. Rev. B: Condens. Matter Mater. Phys.* **2006**, *73*, 193310−193314. Demchak, R. J.; Fort, J. R. T. *J. Colloid Interface Sci.* **1974**, *46*, 191−202

Scheme 2. Synthetic Route for the Assembly of Chromophoric Monolayer. Step 2: Chromophore Anchoring via Quaternization, S_N2 Reaction

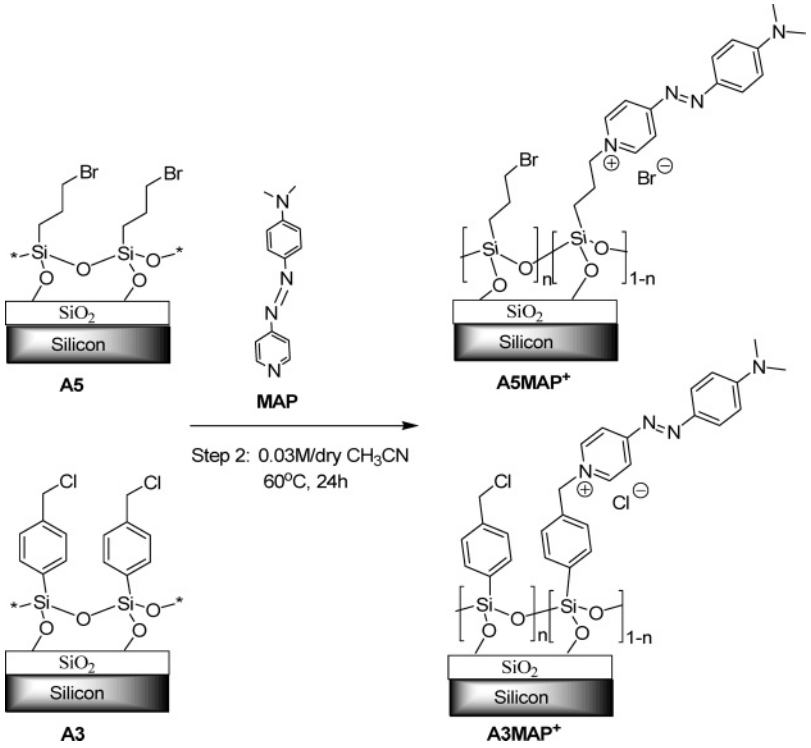

2H), 7.96−7.98(dd, HAr, 2H), 8.06−8.08(d, HAr, 2H), 9.43−9.45(d, HAr, 2H). UV−vis. $\lambda_{max}^{EtOH} = 558$ nm, $\epsilon^{\lambda_{max}}$ (MeOH) = 54 214 [cm^{-1} M^{-1}]. Anal. Calcd: 68.15 C, 6.01 H, 15.91 N. Found: 66.88 C, 6.17 H, 15.45 N.

C. SAM Preparation. C.1. General Synthetic Procedure for Silylated SAMs (Scheme 1). Freshly cleaned Si/SiO_2 (silicon's native oxide) or glass substrates were immersed in a 1% (v/v) coupling agent/hexane solution for 20 min under inert conditions in a Schlenk-line system. Upon completion of the reaction, the substrates were washed three times with dry hexane under inert conditions, sonicated for 1 min in acetone in order to remove any excess of coupling agent, and allowed to dry in an oven at 110 °C for about 15 min.

C.2. Monolayer Functionalization with Azo-Containing Chromophore, Pyridinium Salt, MAP$^+$ (Scheme 2). The silylated surfaces with terminal halide groups were dipped in dry acetonitrile ~0.03 M MAP solution at 70 °C for 24 h. In order to tune the chromophores' surface number density, the substrates were monitored at different reaction times and characterized both electrically and by spectroscopy after washing with IPA and nitrogen drying.

D. Instrumentation. AFM measurements were carried out with a Nanoscope IV (DI) in tapping mode using a tapping etched silicon probe (TESP, DI) with a 30 N/m force constant. All substrates were imaged in air. UV−vis spectra were acquired on a Shimadzu UV-3101PC spectrophotometer using glass substrates. Contact angle measurements were performed using Si substrates with a FTA125 video-based contact angle meter (first 10 Å). XPS spectra were collected at ultrahigh vacuum (2.5×10^{-10} Torr) on a 5600 Multi-Technique (AES/XPS) system (PHI) using an X-ray source of Al K (1486.6 eV). VASE measurements were carried out on a VB-200 ellipsometer (Woollam Co.) around the Brewster angle of Si (75°). CPD measurements were conducted using an Au grid (Kelvin probe S, DeltaPhi Besocke, Jülich, Germany) that vibrates by a piezoelectric crystal. In order to measure the V_{CPD} value, a semiconductor sample, with InGa Ohmic back contact, is placed parallel to the grid, thus creating a closely spaced parallel plate capacitor. The entire experimental setup was placed in a home-built Faraday cage in an inert atmosphere. Upon electrical connection, equilibrium is reached and then the V_{CPD} value is equal to the difference in the WF of the semiconductor surface and the vibrating Au grid. The vibrating capacitor leads to a time-dependent variation in capacitance which induces an ac current flow through the circuit. By tuning the external dc bias, the compensating V_{CPD} value is determined when the current flow is nullified. Therefore, the change in the semiconductor's WF can be determined. Upon illumination of the semiconductor, electron−hole pairs are generated close to the surface, leading to a decrease in the BB. This reduction of BB upon illumination will continue until the bands become almost flat (photosaturation condition). A quartz tungsten halogen (QTH) lamp, intensity 130 mW cm^{-2}, which was assumed to lead to complete flattening of the bands, was used. The BBwas determined by comparing the CPD value in the dark with the value under intense illumination, where the bands are nearly flat. The CPD measurements were taken after the few minutes needed for the signal to stabilize. In order to eliminate molecule decomposition during photosaturation measurements, we used an optical filter that blocks wavelengths adsorbed by the molecules (Schott, RG-780).

E. Molecular Modeling. The surface dipole Φ_s values for the various coupling agents and for the different chromophore-derived surface dipole densities were extracted from the Helmholtz equation (eq 1). The molecular dipole μ was obtained from MOPAC after minimization (AM1 method on the trimethoxysilanes derivatives as "free" molecule) which gave the dipole value in debye. N and ϵ were taken as average experimental values obtained for halogen-modified aliphatic chains,[44−45] and the tilt angle θ was estimated by ellipsometric measurements to be 20° to the normal.

Results and Disscusion

Coupling-Agent Layers. The various coupling agents discussed in this study (Scheme 1) were self-assembled covalently to the native oxide of Si/SiO_2 substrates and structurally characterized by ellipsometry and contact angle along with CPD electronically (Table 1).

(45) Olivera, O. N.; Taylor, D. M.; Lewis, T. J.; Salvagno, S.; And, Stirling, J. M. *J. Chem. Soc., Faraday Trans. 1* **1989**, *85* (4), 1009−1018.

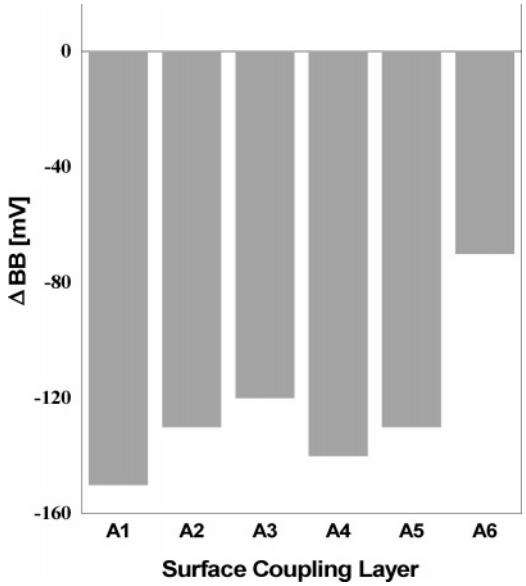

Figure 1. Change in silicon's band-bending (ΔBB) as a function of the various surface functionalities (±10 mV) relative to clean and activated Si substrate.

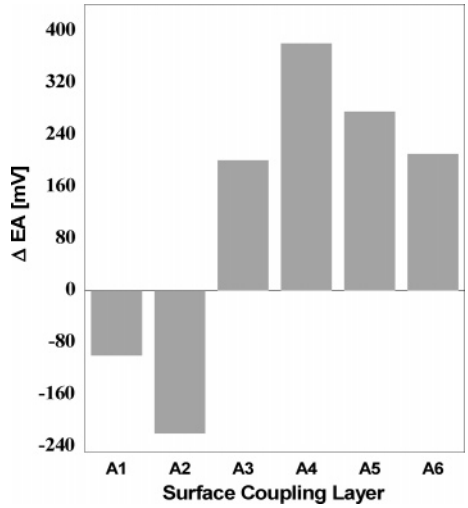

Figure 2. Change in silicon's electron affinity (ΔEA) as a function of the various surface functionalities (±10 mV) relative to clean and activated Si substrate.

Two different parameters affecting the WF of Si were studied: the end group which determines the direction and strength of the molecular dipole and the character of the spacer (aromatic vs aliphatic). As known, the change in WF is directly related to the molecular dipole size and direction arising from the molecules comprising the layer.[46,47] The dipole can be determined experimentally by CPD and theoretically derived from the Helmholtz relation. CPD measurements were conducted by the Kelvin probe technique in order to observe the effect of the different coupling agents on the WF of highly doped n-type Si substrates. In order to enable the separation of the different parameters contributing to the WF (i.e., BB, EA), the sample was illuminated until band flattening was reached. The BB was calculated by subtracting the measured dark value of the WF from the value measured under photosaturation conditions. The EA value was determined by subtracting the BB value from the WF value. We used relative parameters (ΔEA, ΔBB) by subtracting the reference value of the bare Si substrate from that of the modified Si value.

As can be seen in Figures 1 and 2, upon surface functionalization, changes in the BB and EA values can be observed. Regarding the difference in the ΔBB parameter for each coupling agent, (Figure 1), we observed that the major effect is surface-state passivation characterized by a decrease in the BB value, i.e., a negative ΔBB value for all the couplers of about 130 mV (except A6 due to the high polarizability of the end group, as will be discussed below).

It is worth mentioning that upon coupling agent modification, only surface (chemical) passivation occurs. The general value of the change in the BB value can be regarded as originating from the dangling bond that exists at the Si lattice/native oxide interface and from the terminal silanol to siloxane groups ratio of the oxide layer located at the oxide/adsorbed monolayer interface. The coupling agent molecules covalently anchored to the surface affect only the latter due to the fact that the dangling bonds are completely out of reach for creating a covalent bond with the coupling agent molecules. Following surface activation, a maximal density of terminal hydroxyl groups' sites (silanol groups) was obtained in the silicon oxide/air interface, depending strongly on the cleaning and activation method. Therefore, a high number of local negative charges exist on the surface of the n-type Si leading to a high value of BB. The surface condensation reaction that alter the terminal silanol bonds with 2D polysiloxane network bonds eliminates the electron traps (acidic silanol) on the surface, thus significantly diminishing the BB, although there are still unreacted hydroxyl sites. The fact that similar passivation is obtained for various coupling agents indicates that the differences in the number of the unreacted sites are negligible; i.e., similar surface number densities can be estimated. The differences between the ΔBB values for the different coupling agents molecules have to do with their ability to stabilize a negative surface charge on n-type Si. As expected,[12] the smaller effect observed for the iodide group (A6) is related to the ability of this polarizable group to act as an "electron trap," hence, increasing the surface density of states by half. However, the fact that the A6 differs may also arise from the large size of the iodine end group which generates a less dense and organized monolayer, giving a comparatively lower change in BB.

As opposed to the common major passivation effect observed in all the coupling agents' monolayers concerning the ΔBB parameter, two tendencies on the ΔEA parameter can be observed which differ from one molecule to another and can account for the wide tunability range of 600 mV which varies from −220 up to +380 mV for the various coupling agent-derived monolayers (Figure 2).

The first major effect is attributed to the dipole direction on the ΔEA parameter, as can be predicted from the Helmholtz equation (eq 1). Figure 2 shows that the changes in electron affinity are negative values for donor end groups (A1, A2) and positive for acceptor end groups (A3−A6). Donor end groups induce dipole pointing toward the surface, thus facilitating the

(46) Mönch, W. *Semiconductor Surfaces and Interfaces*; Springer: Berlin, 1995.
(47) Nicolini, R.; Vanzetti, L.; Mula, G.; Baratina, G.; Sorba, L.; Franciosi, A.; Peressi, M.; Baroni, S.; Resta, R.; Baldereschi, A.; Angelo, J. E.; Gerberich, W. W. *Phys. Rev. Lett.* **1994**, *72*, 294−297.
(48) Waggner, A. S.; Grinvald, A. *Ann. N.Y. Acad. Sci.* **1977**, *303*, 217−241.
(49) Loew, L. M.; Simpson, L. L. *Biophysical J.* **1981**, *34*, 353−365.
(50) Roscoe, S.; Yitzchaik, S.; Kakkar, K.; Marks, J. T. *Langmuir* **1996**, *12*, 5338−5349.
(51) Yitzchaik, S.; Marks, J. T. *Acc. Chem. Res.* **1996**, *29*, 197−202.

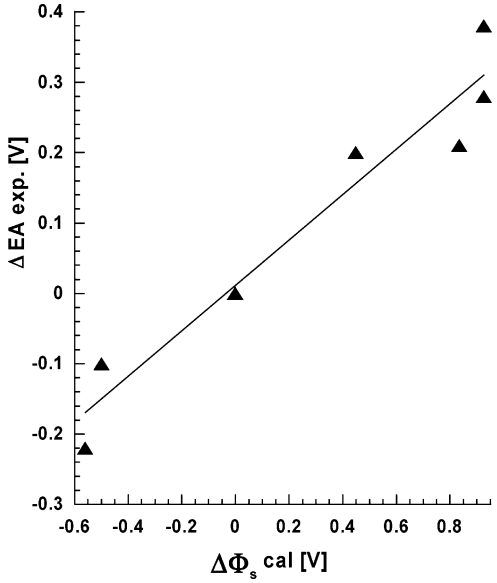

Figure 3. Correlation between experimentally measured change in electron affinity (ΔEA) and surface dipole values (ΔΦ) calculated from the Helmholtz equation for the various coupling layers.

removal of electrons by decreasing the WF. On the other hand, acceptor end groups induce a dipole pointing away from the surface, thus causing an increase in the WF. The other minor effects relate to the differences in the dipoles' magnitude and give insight to the shielding of the aromatic spacer ring compared to the aliphatic spacer. When the dipole magnitude is decreased from A4 to A6 (Table 1), a decrease in the surface dipole is obtained as well. It is noteworthy that although there might be differences in the molecular spatial orientation that can influence the measured ΔEA value, we consider that the densities of all the monolayers obtained (apart from A6) are similar, based on previous studies.[11,52] The ring shielding parameter can be derived by comparison of aromatic and aliphatic spacers with the same end groups (A3, A4). As can be seen, the delocalization of the π electrons shields the effect of the acceptor end group, thus causing a decrease in the surface dipole which is about 200 mV lower than that of the aliphatic spacer. This effect is preserved even after the deposition of another chromophoric layer on the template layer of the coupling agent (vide infra). Figure 3 shows the correlation between the experimental surface dipole value obtained from CPD measurements on modified substrates and the theoretical calculations of couplers' dipoles by the Helmholtz equation.

A linear dependence was obtained between the calculated $\Delta\Phi_s$ values and observed CPD measurements, indicating that the Helmholtz equation describes accurately the change in electron affinity due to monolayer assembly of various molecular dipoles. The Helmholtz equation gives the surface potential drop through a monolayer and is evaluated by using the experimental values of the molecular layer number density and tilt angle including the calculated molecular dipole and dielectric constant of the isolated molecules. The experimental surface potential differs from the calculated one by measuring the effective dielectric constant of the monolayer. The observed deviation from unity slope exhibits the change in the effective dielectric constant induced by these polarizable monolayers.

(52) Malik, A.; Lin, W.; Durbin, M. K.; Marks, T. J.; Dutta, P. *J. Chem . Phys.* **1997**, *107*, 645−652.

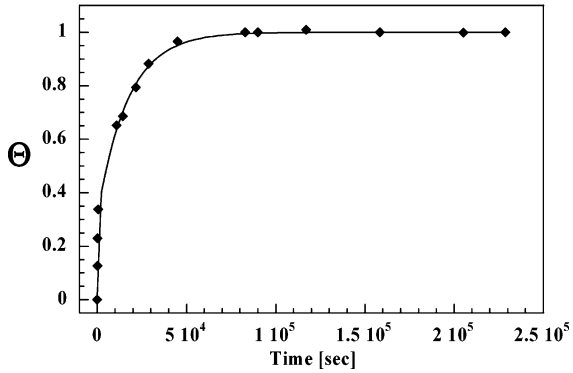

Figure 4. Chromophore anchoring reaction followed by absorption at 550 nm O.D 0.013 for full coverage. Reactions conditions are 0.03 M of MAP in CH_3CN, at 70 °C. The derived biexponential first-order kinetic parameters are $\alpha = 0.314 \pm 0.012$, $k_1 = (7.49 \pm 0.80) \times 10^{-3}$, $k_2 = (5.86 \pm 0.17) \times 10^{-5}$, and $R = 0.9996$.

Chromophoric Layers. Our synthetic approach to chromophoric layer assembly utilizes two coupling agent monolayers with good leaving halogen end groups and similar distances (ca. 7 to 8 Å) from the surface (A3, A5) which can easily undergo S_N2 reaction on the surface (Scheme 2). Our motivation for choosing the MAP chromophore was the fact that this chromophore is known to be a voltage-sensitive dye[48,49] and can be applied in sensors and other devices due to the dipole flipping ability upon excitation. Scheme 2 describes the MAP precursor which undergoes quaternization reaction on the surface from solution while leaving a compensating labile anion upon this surface-anchoring reaction. As shown in Figure 4, full coverage was achieved, creating a chromophoric monolayer assembly which leads to a collective dipole change of the surface. This dipole change consists of molecular dipole due to the formation of covalently attached pyridinium cation and an ionic dipole due to the position of the labile anion relative to the grafted organic cation. In our case, the density of the chromophoric layer (~55 Å^2/molecule) enables the anion to be in the pyridinium plane.[50,51] Since CPD measurements can detect only dipoles which are perpendicular to the surface, in the case where the anion is in the pyridinium' plane (Scheme 2), the major contribution to the dipole density arises from the molecular dipoles. In the case of higher pyridinium density, the anion is constrained to move from the pyridinium plane and the measured CPD value is a summation of both dipoles (this effect will be discussed elsewhere). Upon quaternization, the MAP^+ molecules undergo a bathochromic shift (Supporting Information Figure I) accompanied by band broadening, characteristic of intramolecular charge transfer (CT) absorption. The course of the monolayer assembly was also verified by contact angle, XPS, and ellipsometric measurements (see the Supporting Information).

The maximal surface coverage of the chromophoric layer was found to be 1.8×10^{14} molecules/cm^2, based on absorption spectroscopic analysis at a wavelength of 550 nm (λ_{max}). Figure 4 demonstrates the quaternization reaction kinetics, confirming full surface coverage with kinetic parameters similar to those reported for the related stilbazolium chromophore.[51]

$$(1 - \theta) = \alpha e^{-k_1 t[C]} + (1 - \alpha) e^{-k_2 t[C]} \qquad (2)$$

The successful biexponential fit observed here provides a real indication that the self-assembling quaternization must be

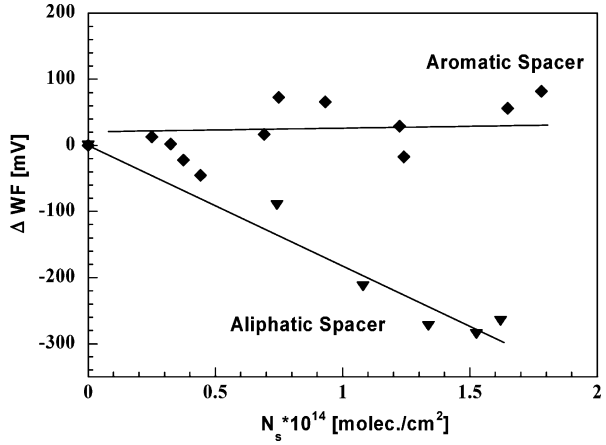

Figure 5. Change in silicon WF relative to the relevant coupling agent-modified substrate, as a function of MAP^+ surface number density on aromatic A3 (diamonds) and aliphatic A5 (triangles) templates (±10 mV). *The curves are drawn as guides to the eye.* The zero point describes the WF for zero chromophoric coverage for both coupling agents.

described by more than one rate process ("fast" and "slow" rate constants). The slower rate k_2' is likely associated with increasing repulsive interactions between adsorbed molecules at higher coverage. Upon grafting a chromophore on a coupling agent position, a change in the dipole orientation occurs; i.e., dipoles that were pointing out of the surface (coupling agents, A3, A5) alter their dipole direction. Thus, increasing the chromophoric monolayer density will lead to more dipoles pointing toward the surface. In order to reach chromophoric submonolayer densities, different incubation times in chromophoric solution were measured for the coupling agent-modified substrate (Scheme 2). In that way we controlled the chromophore number density on the surface by reacting different numbers of alky- or benzyl-halide sites on the surface via solution assembly. It would be expected that the magnitude of the change in WF would increase upon increasing chromophoric layer density versus the coupling layer-modified Si (Figure 5). However, this trend was observed only for the MAP^+ monolayer built on an aliphatic coupling agent (A5-MAP^+), while on the aromatic coupling agent (A3-MAP^+) there seems to be no dependence of the WF on the chromophore number density (Figure 5, aromatic). In order to explain this fact we isolated each parameter contributing to the change in the WF (i.e., ΔBB and ΔEA).

For A3, the aromatic coupling agent, a positive value of ΔEA (+200 mV) was obtained due to the coupling agent's surface modification (Figure 2). Upon grafting mounting densities of the chromophoric monolayer MAP^+ on A3 sites, the surface dipole density grows, leading to a ΔEA value of −200 mV for full surface coverage (∼55 Å^2/molecule) as can be seen in Figure 6. In addition, by increasing the chromophoric monolayer density, more electron traps are introduced on the surface, causing a depletion layer due to an increase of local negative charge concentration on the n-type Si surface. This effect is observed by the change in the ΔBB value from −120 mV upon coupling agents' passivation to +200 mV upon full chromophoric monolayer coverage. It can be seen that the net result of a summation of the ΔBB and ΔEA values is nearly annealed (Figure 5, aromatic).

For maximal surface number density of chromophoric monolayer (∼55 Å^2/molecule) grafted upon an A5 coupling agent

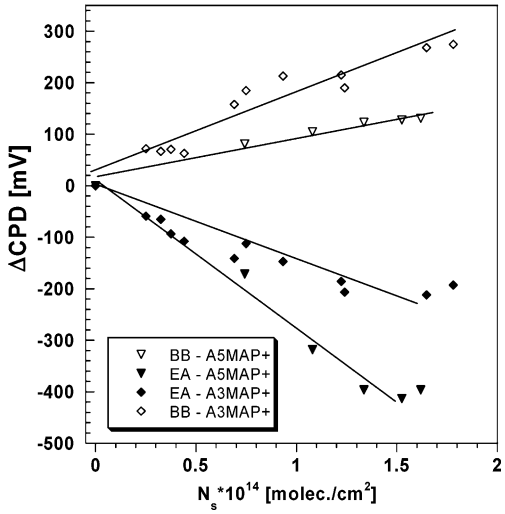

Figure 6. Change in electron affinity (ΔEA) and band bending (ΔBB) parameters (±10 mV) relative to the relevant coupling agent-modified substrate, as a function of the chromophore surface number density on aromatic (A3) and aliphatic (A5) coupling agents containing SAMs. *The curves are drawn as guides to the eye.* The zero point describes the ΔCPD value for zero chromophoric coverage for both coupling agents.

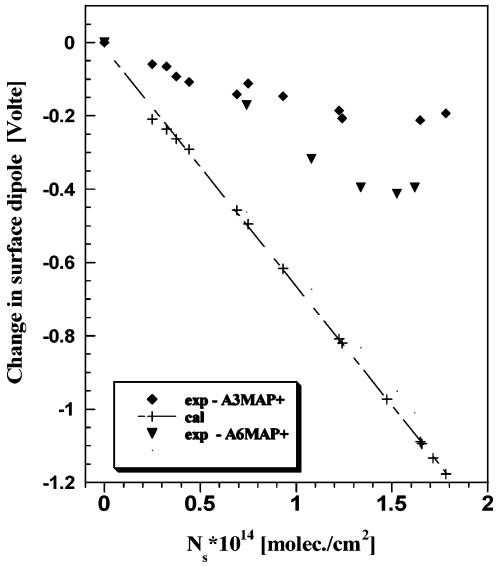

Figure 7. Change in calculated (+) and experimentally measured surface dipole relative to the relevant coupling agent-modified substrate, as a function of chromophore surface number density on aromatic (◆) and aliphatic (▼) spacers containing monolayers. The zero point describes the ΔEA value for zero chromophoric coverage for both coupling agents.

monolayer, a value of −420 mV was obtained for the ΔEA. The difference in the ΔEA values for the same chromophore and surface density can be accounted for the shielding parameter due to the aromatic ring, as was shown for coupling agent modifications (∼200 mV). A positive value in the ΔBB is obtained due to an increase in electron traps sites upon grafting the chromophoric monolayer. The value obtained in this case is smaller than the one obtained for the aromatic spacer due to the lack in aromatic rings, which can serve as traps for electrons as well.

Figure 7 shows the dependence of the change in the calculated and measured surface dipole as a function of chromophore surface number density. The change in surface dipole was calculated by putting the calculated molecular dipole value into the Helmholtz equation and comparing it with the measured

CPD values. It can be seen that for the calculated values there is a linear fit between the surface dipole and the coverage, as expected for increasing chromophore number densities. As opposed to that result, the measured values give saturated curves, indicating a global effect of monolayer' dipole depolarization, as expected for such a high molecular dipole packed densely.

Conclusion

We have shown a way to systematically control the surface and interface electronic properties of an oxide-bearing silicon by the use of an organic monolayer. Two parameters seem to be of major importance: the first one is the molecular dipoles of the surface anchored molecule and the other one is the surface coverage of the substrate. A secondary effect concerned the spacer type used for the coupling of the inorganic substrate and the organic monolayers. It was shown that an aromatic spacer gives rise to a shielding effect of the ring that can be estimated to be about 200 mV and which diminishes the electronic effect when compared with an aliphatic spacer of the same length. This effect originates from the larger effective dielectric constant of the aromatic spacer. Due to that observation, it seems to be more efficient for further applications in devices to use aliphatic spacers which do not shield the effect of the added monolayers' dipole on the substrate. Concerning the chromophoric layer obtained in the second step (Scheme 2), it was clearly shown that upon increasing surface chromophoric coverage an increase in the electronic properties was observed. However, a major effect of depolarization was observed on both coupling template layers. On the basis of this observation, it can also be concluded that in order to get a high surface dipole it is better to use molecules with lower value molecular dipoles which can form a more ordered and dense monolayer with low depolarization affects than to use a molecule with a very high value molecular dipole that undergoes large depolarization in the layer. In any case, it is clear that when increasing the surface coverage, the influence on the surface dipole increases.

Acknowledgment. We thank Dr. Noemi Zenou for helpful and illuminating discussions. This work was supported by the EC through contract FP6-029192 ("DNA-Based Nanodevices").

Supporting Information Available: Model chromophores UV−vis spectroscopy and monolayers characterization by XPS, VASE, and UV−vis spectroscopy. This material is available free of charge via the Internet at http://pubs.acs.org.

JA077933G